Chinese Chemical Letters 37 (2026) 111236

Contents lists available at ScienceDirect

Chinese Chemical Letters

journal homepage: www.elsevier.com/locate/cclet

Plasma metabolites-based drug design: Discovery of novel and highly selective phosphodiesterase 5 inhibitors

Deyan Wu[a,1,*], Qingjiang Ma[a,1], Yanquan Chen[b,1], Guofeng Yang[a], Fengcai Zhang[b], Meiyan Jiang[b], Xue Wang[a], Xingfu Liu[a], Qian Zhou[a], Yi-You Huang[a], Zhe Li[b,*], Hai-Bin Luo[a,*]

[a] Key Laboratory of Tropical Biological Resources of Ministry of Education, School of Pharmaceutical Sciences, Hainan University, Haikou 570228, China
[b] School of Pharmaceutical Sciences, Sun Yat-sen University, Guangzhou 510006, China

ARTICLE INFO

Article history:
Received 17 February 2025
Revised 20 April 2025
Accepted 21 April 2025
Available online 22 April 2025

Keywords:
Drug discovery
Scaffold hopping
High selectivity
Phosphodiesterase 5 inhibitors
Idiopathic pulmonary fibrosis

ABSTRACT

In drug discovery, it is extremely important to identify highly potent leads with desirable drug-like profiles. Almost all the marketed phosphodiesterase 5 (PDE5) inhibitors such as sildenafil, vardenafil, and tadalafil have poor selectivity over PDE6 or PDE11 and leading to several side effects. Herein, a metabolites-based scaffold hopping strategy was performed to discover selective PDE5 inhibitors with remarkable metabolic stability. The $Eu(OTf)_3$-catalyzed Mannich-type reaction followed by L-selectride catalyzed reduction was used to prepare chiral 2,3,3*a*,4,5,6-hexahydro-1*H*-benzo[*b*]pyrido[2,3,4-*de*][1,6] naphthyridines as novel PDE5 inhibitors with high enantioselectivity (>99% *ee* and >30:1 *dr*). Lead **L9** exhibited a half maximal inhibitory concentration (IC_{50}) of 1.03 nmol/L with higher selectivity (>898-fold) over PDE6 or PDE11 than sildenafil and tadalafil, implying the potential relief from side effects. Especially, the co-crystal binding pattern of **L9** with PDE5 is revealed to be different from that of sildenafil, which possibly explain the former's high selectivity. And oral administration of **L9**·HCl (5.0 mg/kg) exhibited better therapeutic effects than pirfenidone (150 mg/kg) in a bleomycin-induced idiopathic pulmonary fibrosis (IPF) rat model, highlighting the potential of **L9**·HCl for the treatment of IPF.

© 2026 Published by Elsevier B.V. on behalf of Chinese Chemical Society and Institute of Materia Medica, Chinese Academy of Medical Sciences.

One of the biggest challenges in the drug discovery is to identify the high-quality hit or lead compounds. In general, early drug discovery and development usually starts with accidental discovery and natural product [1]. With the improvements in drug development strategies the new drug screening methods have emerged and always played an important role [2,3], such as structure-based drug design (SBDD), fragment-based drug discovery (FBDD), high-throughput screening, scaffold hopping, biocatalysis, structural biology, and artificial Intelligence techniques [4–6]. However, the fate of a drug depends on each other administration in the body involves absorption, distribution, metabolism, and excretion (ADME), which is a complex biotransformation process [7,8]. Therefore, the metabolization characteristics of the drug on pharmacokinetics (PK), pharmacodynamics (PD), and safety should be carefully considered.

There are generally accepted rules were effectively applied to improving PK and PD properties, such as structural modification on or around the metabolic soft spots [9,10], metabolic switching and deuterium replacement [11,12], prodrugs or active metabolites as new drug candidates [4,13,14], minimizing toxicity potential associated with bioactivation [13,14], and the machine learning techniques improve the decision-making in drug discovery in recent years [15,16], but the structure-metabolism relationships of the drug is complex and still not completely understood [7]. Therefore, new strategies for drug discovery still need to be discovered.

Idiopathic pulmonary fibrosis (IPF) is a chronic, progressive and irreversible interstitial lung disease and effective therapy is lacking that resulting in a median survival of only 2.5–3.5 years after diagnosis [17–21]. However, effective therapy for IPF is still lacking, and only two anti-fibrotic drugs (pirfenidone and nintedanib) are available to delay the disease progression [22–25]. Sildenafil, a phosphodiesterase 5 (PDE5) inhibitor, has already used in anti-IPF study [26,27], but it has poor selectivity of 10-fold over PDE6 and leading to several side effects [28,29]. Moreover, almost all of the currently marketed PDE5 inhibitors (such as sildenafil, vardenafil, and tadalafil) existing of these common side effects [28]. Sildenafil, vardenafil, and avanafil results in the visual side effects by inhibiting PDE6 [28,30]. Tadalafil, on the other hand, is selective *versus* PDE6, but potently inhibits PDE11 which result in the back

* Corresponding authors.
E-mail addresses: wudeyan@hainanu.edu.cn (D. Wu), lizhe5@mail.sysu.edu.cn (Z. Li), hbluo@hainanu.edu.cn (H.-B. Luo).
[1] These authors contributed equally to this work.

https://doi.org/10.1016/j.cclet.2025.111236
1001-8417/© 2026 Published by Elsevier B.V. on behalf of Chinese Chemical Society and Institute of Materia Medica, Chinese Academy of Medical Sciences.

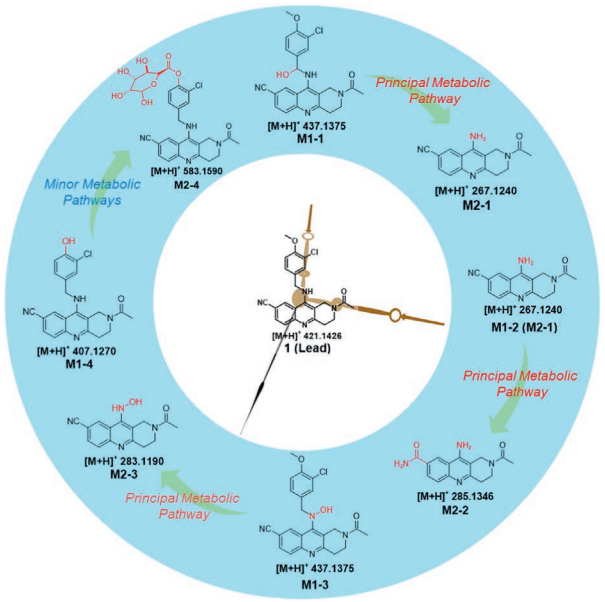


Fig. 1. Metabolite analysis of the hit compound reveals that the "*N*-(3–chloro–4-methoxybenzyl)" group was the metabolic soft spots.

and muscle pain [28]. Therefore, the discovery of novel selective PDE5 inhibitors with improved safety profiles would be a welcome contribution to drugs study.

Herein, we reported a metabolites-based scaffold hopping strategy with the absolute binding free energy calculation for the discovery of 2,3,3*a*,4,5,6-hexahydro-1*H*-benzo[*b*]pyrido[2,3,4-*de*][1,6]naphthyridines as novel and highly selective PDE5 inhibitors with remarkable metabolic stability for the treatment of IPF. In this study, the hit compound (**1**) with a 1,2,3,4-tetrahydro benzo[*b*][1,6]naphthyridine scaffold and exhibited potent inhibitory activity as well as excellent selectivity, whereas it was unstable in rat liver microsomes with the $t_{1/2}$ of 3.2 min [31]. And the subsequent metabolic studies shows that the "*N*-(3–chloro–4-methoxybenzyl)" group was the metabolic soft spots (Fig. 1 and Table S1 in Supporting information).

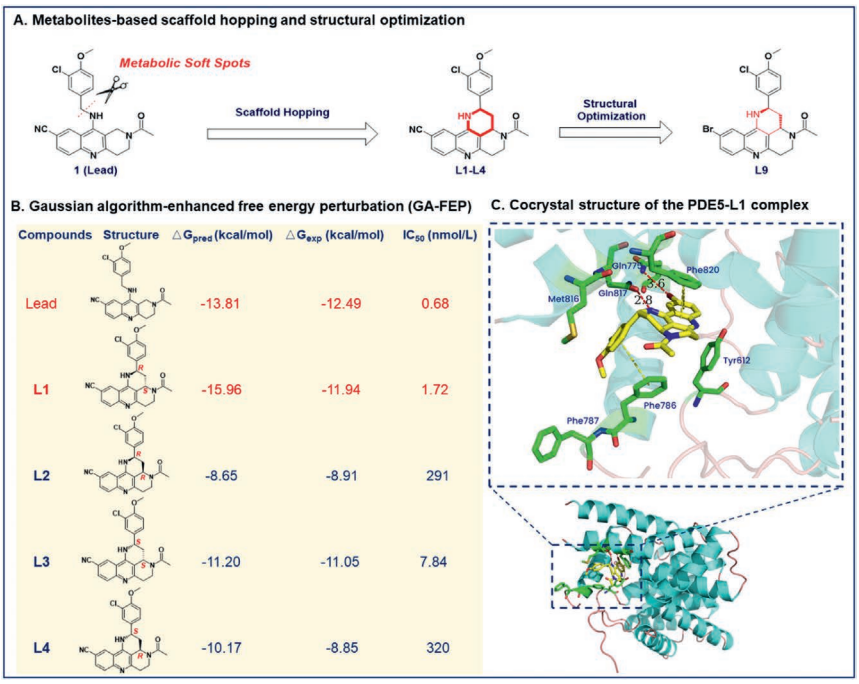
In order to achieve the goal of discovering highly potent and selective PDE5 inhibitors with reasonable drug-like properties, a "2,3,3*a*,4,5,6-hexahydro-1*H*-benzo[*b*]pyrido[2,3,4-*de*][1,6]naphthyridine" scaffold was designed to blocking the metabolic sites of **1** *via* cyclizing the *N*-(3–chloro–4-methoxybenzyl) motif to the 1,2,3,4-tetrahydrobenzo[*b*][1,6] naphthyridines (Scheme 1A). Following the liver microsomal stability study show that the novel compound **L1** have a dramatic improvement on the metabolic stability with $t_{1/2}$ of 139 min. It is worth mentioning that we have developed an innovative drug design method, a Gaussian algorithm-enhanced free energy perturbation (GA-FEP) protocol [32–34], which has been used in this study to discover highly potent PDE5 inhibitors (Scheme 1B). In addition, their predicted binding patterns were further verified by determining a cocrystal structure of the PDE5-inhibitor complex (Scheme 1C), and the predicted binding free energies correlate well with the experimental activity data (Scheme 1B).

However, these chiral 1,2,3,4-tetrahydrobenzo[*b*][1,6]naphthyridines has not been explored. In this study, we wish to disclosure a concise and efficient method for the preparation of chiral 2,3,3*a*,4,5,6-hexahydro-1*H*-benzo[*b*]pyrido[2,3,4-*de*][1,6] naphthyridines as novel PDE5 inhibitors with high enantioselectivity (>99% *ee* and >30:1 *dr*) and good yields which highlighted the utility of a $Eu(OTf)_3$-catalyzed Mannich-type reaction for constructing the key scaffolds (Scheme 2). Specifically, by use 10–chloro–3,4-dihydrobenzo[*b*][1,6]naphthyridine-8-carbonitrile (**1**) and ((1-(3–chloro–4-methoxyphenyl)vinyl)oxy)trimethylsilane (**2**) as the starting materials and treated with $Eu(OTf)_3$ or $Sc(OTf)_3$ in dichloromethane to get the key compound **3**. Then acetylation of the amine **3** to afford the ketone **4**. This intermediate is a reactive electrophilic reagent that readily react with the chiral *tert*–butanesulfinamide [35] resulting in afforded sulfonamides (**5**) and make the separation of the diastereoisomers easier by column chromatography, respectively. After separation of the diastereomers, an L-selectride catalyzed highly enantioselective reduction reaction [36] was conducted to afford the functionalized chiral amines (**6**), respectively. Finally, an intramolecular cyclization of the amines **6** giving the target compounds **L1–4** with high enantioselectivities (>99% *ee* and >30:1 *dr*) and high yields, respectively. Under optimized reaction conditions and for the purpose of further explore the structure−activity relationships around the novel scaffold, derivatives **L5–10** were synthesized (Scheme 3). The results of exploratory studies have demonstrated that the $Eu(OTf)_3$-catalyzed Mannich-type reaction followed by L-selectride catalyzed reduction serves as an effective method for the preparation of useful chiral 2,3,3*a*,4,5,6-hexahydro-1*H*-benzo[*b*]pyrido[2,3,4-*de*][1,6] naphthyridines.

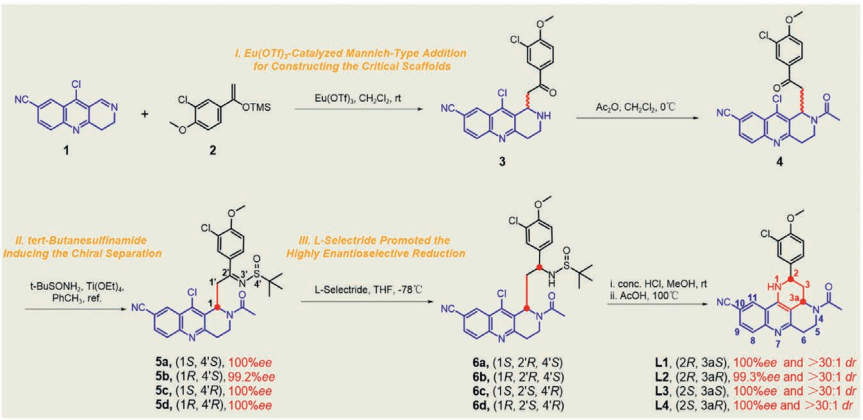
As a result, ten 2,3,3*a*,4,5,6-hexahydro-1*H*-benzo[*b*]pyrido[2,3,4-*de*][1,6]naphthyridines were successfully synthesized with excellent enantioselectivity (>99% *ee* and >30:1 *dr*) and potent inhibitory activities against PDE5 (Table 1). It is worth mentioning that the hit compound has a half maximal inhibitory concentration (IC_{50}) of 0.68 nmol/L under identical assay conditions, and sildenafil was used as the positive control compound. The results showed that compound **L1** based on scaffold hopping has the equivalent inhibitory potency as the hit compound. However, other configurations of **L1** exhibited the decreased inhibitory activities, especially for the compounds with an 2*S*-configuration (**L3** and **L4**). Further investigation revealed that the -CN group may be replaced with a -Br or -Cl group (**L1**, **L8**, and **L9**), while the -Br group exhibited the better inhibitory activities. However, other modifications, such as replacement of a 3–chloro–4-methoxyphenyl group with a benzo[*d*][1,3]dioxol-5-ylmethyl group (**L6**) or a phenyl group (**L10**) exhibited weaker PDE5 inhibitory activities than compound **L9**. Finally, **L9** exhibited highly potent inhibitory activity against PDE5 with the IC_{50} of 1.03 ± 0.03 nmol/L was selected as the potent inhibitor for subsequent study.

Given the highly potent activities of compound **L9**, we measured the selectivity index (SI) across phosphodiesterase (PDE) subtypes. Under identical assay conditions, **L9** have a SI of 898-fold against PDE6, and the SI values against PDE1, PDE2, PDE3, PDE4, PDE7, PDE8, PDE9, PDE10, PDE11 were uniformly greater than 1000-fold (Table 2). These results suggest that **L9** exhibited at least 898-fold selectivity over other PDE families (Table 2). It is worth mentioned is sildenafil only has a SI of 8∼10-fold against PDE6 [28,37–41], while tadalafil only has a SI of 5∼9-fold against PDE11 (Table 2) [28,37]. Therefore, the study discovered 2,3,3*a*,4,5,6-hexahydro-1*H*-benzo[*b*]pyrido[2,3,4-*de*][1,6]naphthyridines as novel PDE5 inhibitors with higher selectivity over other PDE families, especially for PDE6 and PDE11, which is of great significance in the potential relief of several side effects.

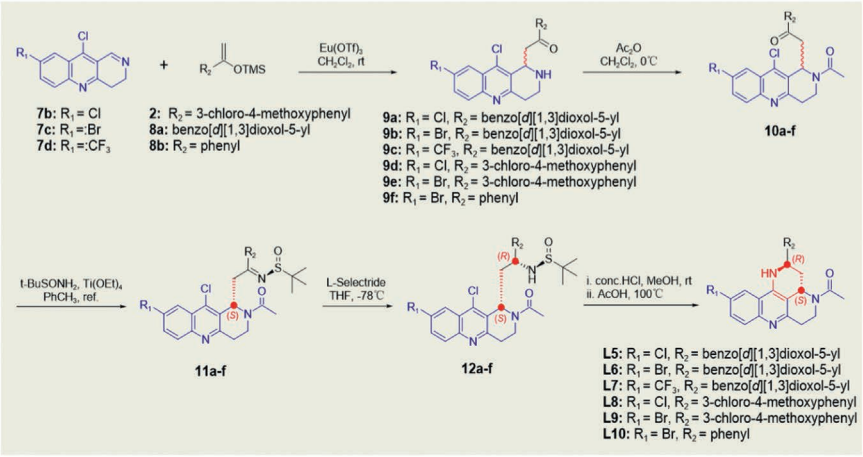
The co-crystals further revealed that 2,3,3*a*,4,5,6-hexahydro-1*H*-benzo[*b*]pyrido[2,3,4-*de*][1,6]naphthyridines had a specific binding pattern. In this study, the cocrystal structures of PDE5 with **L1** and **L9** were successfully determined (PDB ID: 9LSL and 9LSM), respectively. As shown in Fig. 2, the structures indicated that **L1** (Fig. 2A) and **L9** (Fig. 2B) occupies the active pocket with a unique binding pattern. Specifically, each of the NH group formed H-bond with residue Gln817 and the tetracyclic ring formed $\pi-\pi$ stacking interaction with residue Phe820, which are two charac-



Scheme 1. Schematic diagram for the metabolites-based scaffold hopping strategy combined with the absolute binding free energy calculation for the discovery of novel selective PDE5 inhibitors, and cocrystal structure of PDE5-**L1** revealed that the novel scaffold has a suitable binding pattern.

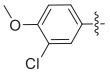
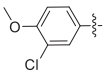
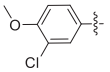
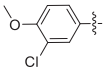
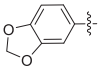
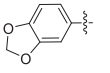
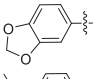
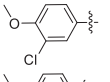
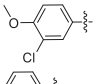


Scheme 2. Synthetic pathway for the production of 2,3,3*a*,4,5,6-hexahydro-1*H*-benzo[*b*]pyrido[2,3,4-*de*][1,6]naphthyridines as novel and highly selective PDE5 inhibitors.



Scheme 3. Synthesis of 2,3,3*a*,4,5,6-hexahydro-1*H*-benzo[*b*]pyrido[2,3,4-*de*][1,6]naphthyridine derivatives.

Table 1
2,3,3*a*,4,5,6-Hexahydro-1*H*-benzo[*b*]pyrido[2,3,4-*de*][1,6]naphthyridines with high enantioselectivity and remarkable inhibitory activities against PDE5.[a]

Compound	R_1	R_2	Stereochemistry	*ee* (%)[a]	*dr*[a]	PDE5, IC_{50} (nmol/L)
Hit	–	–	–	–	–	0.68
Sildenafil[b]	–	–	–	–	–	5.0
L1	-CN		2*R*, 3a*S*	100	>30:1	1.72 ± 0.34
L2	-CN		2*R*, 3a*R*	99.3	>30:1	7.84 ± 0.98
L3	-CN		2*S*, 3a*S*	100	>30:1	291 ± 16
L4	-CN		2*S*, 3a*R*	100	>30:1	320 ± 27
L5	-Cl		2*R*, 3a*S*	100	>30:1	16.1 ± 1.1
L6	-Br		2*R*, 3a*S*	99.2	>30:1	19.9 ± 1.5
L7	$-CF_3$		2*R*, 3a*S*	100	>30:1	276 ± 26
L8	-Cl		2*R*, 3a*S*	100	>30:1	16.4 ± 0.8
L9	-Br		2*R*, 3a*S*	100	>30:1	1.03 ± 0.03
L10	-Br		2*R*, 3a*S*	100	>30:1	47.2 ± 6.2

[a] Determined by chiral HPLC analysis (Opti-Chiral A1–5).
[b] Sildenafil, the reference compound.

Table 2
2,3,3*a*,4,5,6-Hexahydro-1*H*-benzo[*b*]pyrido[2,3,4-*de*][1,6]naphthyridines with high enantioselectivity and remarkable inhibitory activities against PDE5.[a]

PDE isozyme	**L9**		Sildenafil[a]		Tadalafil[a]	
	IC_{50} (nmol/L)	SI	IC_{50} (nmol/L)	SI	IC_{50} (nmol/L)	SI
PDE5	1.03 ± 0.03	–	4.31 ± 0.46	–	2.35 ± 0.28	–
PDE1	>10,300	>10,000	819 ± 89	190	>10,000	>4255
PDE2	>10,300	>10,000	>10,000	>2320	>10,000	>4255
PDE3	>10,300	>10,000	>10,000	>2320	>10,000	>4255
PDE4	>1030	>10,000	>10,000	>2320	>10,000	>4255
PDE6	924.5	898	36.4 ± 1.8	8	402 ± 56	171
PDE7	>10,300	>10,000	>10,000	>2320	>10,000	>4255
PDE8,	>10,300	>10,000	>10,000	>2320	>10,000	>4255
PDE9	>10,300	>10,000	>10,000	>2320	>10,000	>4255
PDE10	>10,300	>10,000	>10,000	>2320	>10,000	>4255
PDE11	>1030	>1000	4930 ± 1140	1144	22.1 ± 5.9	9

[a] The PDE selectivity data of the reference drugs from Ref. [35].

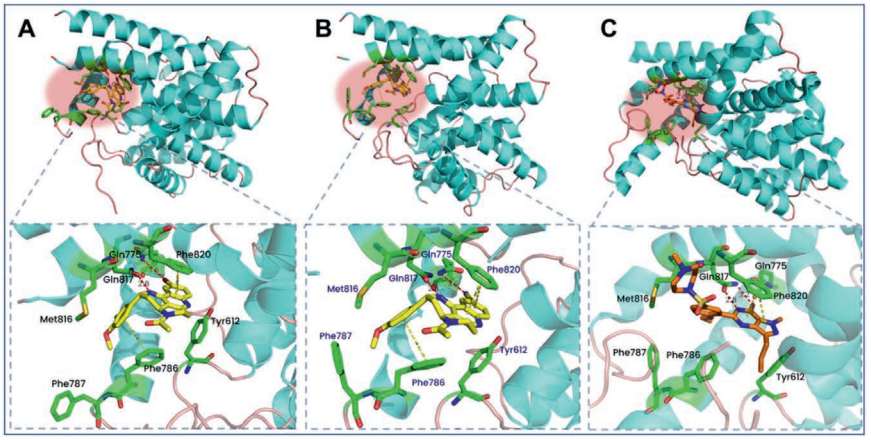


Fig. 2. Cocrystal structures of the PDE5-**L1** and PDE5-**L9** complexes (PDB codes 9LSL and 9LSM): (A) surface model of **L1** with PDE5; (B) surface model of **L9** with PDE5; (C) surface model of sildenafil with PDE5. The dotted lines refer to H-bonds (red) or $\pi-\pi$ stacking interactions (yellow).

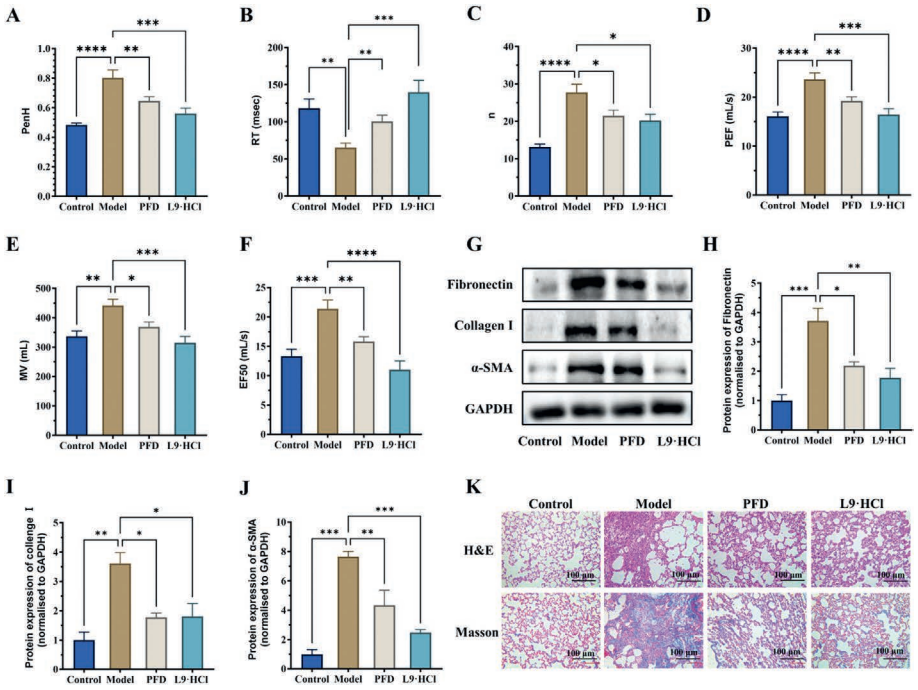


Fig. 3. Anti-IPF effect of **L9**·HCl in a BLM-induced rat model. (A–F) Indicators of the pulmonary respiratory function in different groups of rats. Rats in each group: $n = 12$. (G–J) Western blot analysis of FN, collagen I, and α-SMA protein expression levels [relative to glyceraldehyde 3-phosphate dehydrogenase (GAPDH)] ($n = 3$). (K) The representative image of H&E strain and Masson strain. Scale bar: 100 μm. Data are shown as means ± SEM. $^{*}P < 0.05$, $^{**}P < 0.01$, $^{***}P < 0.001$, $^{****}P < 0.0001$.

teristic interactions of the reported PDE5 inhibitors (*e.g.*, sildenafil, Fig. 3C). However, the -CN group of **L1** or bromine of **L9** formed another H-bond with residue Gln775, and the 3–chloro–4-methoxyphenyl group occupies the small pocket lined by Phe786, Phe787, Leu804, and Met816. These interactions were not observed in the binding pattern of PDE5/sildenafil (Fig. 3C), interpreting that 2,3,3*a*,4,5,6-hexahydro-1*H*-benzo[*b*]pyrido[2,3,4-*de*][1,6]naphthyridines exhibited higher selectivity.

Since compounds exhibited potent activities against PDE5 and highly selectivity over other PDEs, its drug-like profile evaluations were performed. We examined the metabolic stability of designed compounds using a standard microsomal stability assay. The results indicate that **L1** and **L9** made a dramatic improvement on the metabolic stability with the $t_{1/2}$ of 139 and 79 min than the hit **1** of 3.2 min, respectively. In this study, the inhibitory activities of compound **L9** against human hepatic CYP enzymes (Table S3 in Supporting information) were tested. And the results shows that **L9** has an IC_{50} of 2.2 μmol/L against CYP1A2, and its IC_{50} values for the other CYPs (CYP2C9, CYP2C19, CYP2D6, and CYP3A4) were uniformly >25 μmol/L, suggesting that **L9** exhibited a very weak inhibitory effect on these CYP isoenzymes. Besides, compound **L9** inhibited the human ether-à-go-go-related gene (hERG) with an IC_{50} of 0.18 μmol/L using an automated patch clamp electrophysiology measurement in CHO-hERG cells (Fig. S1 in Supporting information). The results suggest that **L9** have a moderate inhibitory effect on hERG.

In terms of the reasonable druglike properties and higher selectivity of **L9**, its pharmacokinetic profile assessment in Sprague Dawley rats after oral administration (po) and intravenous administration (iv) of **L9**·HCl were performed. Note that all animal care and experimental programs were in line with the "Guide of Laboratory Animals" (National Institutes of Health Publication, revised 1996, No. 86–23, Bethesda, MD) and approved by the Institutional Ethical Committee for Animal Research of Sun Yat-sen University (No. SYSU-IACUC-2021–000184). As a result, compound **L9**·HCl exhibited favorable pharmacokinetic properties, and its pharmacokinetic data are summarized in Table 3. After oral administration of a 5.0 mg/kg dose of **L9**·HCl to rats, pharmacokinetic analysis revealed it have a $t_{1/2}$ of 3.79 ± 0.41 h, C_{max} of 119 ± 11.5 ng/mL, area under curve ($AUC_{(0\text{-}t)}$) of 1227 ± 161 ng h mL^{-1} and oral bioavailability of 47.2 %, indicating that it could give a reasonable blood exposure (Table 3). On the basis of its pharmacokinetic profile, compound **L9**·HCl was further subjected to pharmacodynamics studies *in vivo*.

The therapeutic results of **L9**·HCl as anti-IPF agents *in vivo* are shown in Fig. 3, the pulmonary function parameters of rats in the blcomycin (BLM)-induced model group, including enhanced pause (penH), respiratory rate (n), peak expiratory flow (PEF), and mid-expiratory flow (EF_{50}) remarkably increased compared with those in the control group, indicating that the BLM-induced IPF model was successfully established. After 28 consecutive days of oral administration, compound **L9**·HCl had remarkable efficacy in improving the lung function of IPF rats in terms of those parameters such as EF_{50}, PEF, and penH reverted to resemble those in the control group (Figs. 3A–F). As a result, **L9**·HCl at an oral dose of 5.0 mg/kg had better anti-IPF effect than the marketed drug pirfenidone (PFD) administered at an oral dose of 150 mg/kg. Usually, collagen deposition was one of key pathological features in IPF, both **L9**·HCl and PFD almost completely inhibited collagen deposition to a normal level in this study. The expression levels of the fibronectin (FN), collagen I, and α-smooth muscle actin protein (α-SMA) in the lung tissue, the marker proteins in IPF, were upregulated in the model group relative to those in the control group as determined by Western blot (Figs. 3G–J). And **L9**·HCl and PFD significantly decreased the levels of FN, collagen I, and α-SMA. Hematoxylin and eosin (H&E) staining showed disordered alveoli, ruptured alveolar walls, and apparent inflammatory cell infiltration in the lung tissues of the model group (Fig. 3K). **L9**·HCl (5.0 mg/kg) and PFD (150 mg/kg) could both effectively alleviate this structural damage to the lungs with fewer fibrotic lesions. Besides, blue staining indicated that the expression of collagen deposition was greatly increased with large areas of collagen deposition around the trachea and cell hyperplasia in the model group (Fig. 3K). These results demonstrated that the PDE5 inhibitor **L9**·HCl ameliorated the BLM induced pulmonary fibrosis.

Table 3
Pharmacokinetic profile of **L9**·HCl in rats.

Route	$t_{1/2}$ (h)	t_{max} (h)	C_{max} (ng/mL)	$AUC_{(0\text{-}t)}$ (ng h mL^{-1})	$AUC_{(0\text{-}\infty)}$ (ng h mL^{-1})	$MRT_{(0\text{-}t)}$ (h)[a]	F (%)
po (5.0 mg/kg)	3.79 ± 0.41	4.67 ± 2.31	119 ± 11.5	1227 ± 161	1249 ± 170	6.54 ± 0.34	47.2 ± 0.01
iv (2.5 mg/kg)	4.56 ± 0.34	0.083 ± 0.00	363 ± 56.5	1295 ± 130	1323 ± 138	4.67 ± 0.02	

[a] MRT: mean residence time.

In conclusion, one of the biggest challenges in the drug discovery is to identify the highly potent hit or lead compounds with remarkable safety and pharmacokinetic profiles. Until now, almost all of the currently marketed PDE5 inhibitors (such as sildenafil, vardenafil, and tadalafil) have poor selectivity over PDE6 or PDE11, which leads to several side effects. In the study, a metabolites-based scaffold hopping strategy with the absolute binding free energy calculation was used to discover highly selective PDE5 inhibitors with remarkable metabolic stability from the starting compound **1** with a poor $t_{1/2}$ of 3.2 min. It is worth noting that the $Eu(OTf)_3$-catalyzed Mannich-type reaction followed by L-selectride catalyzed reduction serves as an efficient method for preparation of useful chiral 2,3,3*a*,4,5,6-hexahydro-1*H*-benzo[*b*]pyrido[2,3,4-*de*][1,6]naphthyridines as novel PDE5 inhibitors with high enantioselectivity (>99% *ee* and >30:1 *dr*) and high selectivity over other PDE subtypes. Further investigation of the scope of the cascade reaction and 10 derivatives of 2,3,3*a*,4,5,6-hexahydro-1*H*-benzo[*b*]pyrido[2,3,4-*de*][1,6]naphthyridines were discovered, resulting in 7 compounds with an IC_{50} values ranging from 1 nmol/L to 100 nmol/L and 3 compounds with the IC_{50} < 10 nmol/L. The most potent inhibitor **L9** has an IC_{50} of 1.03 ± 0.03 nmol/L with high selectivity (≥898-fold) over other PDEs and oral bioavailability of 47.2%. And oral administration of **L9**·HCl (5.0 mg/kg) exhibited better anti-pulmonary fibrotic effects than the reference compound pirfenidone (150 mg/kg) in a bleomycin-induced IPF rat model, indicate that **L9**·HCl is a potential lead for the treatment of IPF.

In short, the strategies for improving both inhibitor selectivity against other isoforms and metabolic stability discussed above may be applicable for other drug discovery programs.

Declaration of competing interest

The authors declare that they have no known competing financial interests or personal relationships that could have appeared to influence the work reported in this paper.

CRediT authorship contribution statement

Deyan Wu: Writing – review & editing, Writing – original draft, Validation, Software, Resources, Formal analysis. **Qingjiang Ma:** Methodology, Investigation, Conceptualization. **Yanquan Chen:** Methodology, Investigation, Formal analysis, Data curation. **Guofeng Yang:** Methodology, Investigation, Formal analysis, Data curation. **Fengcai Zhang:** Methodology, Investigation, Formal analysis. **Meiyan Jiang:** Methodology, Investigation. **Xue Wang:** Investigation, Formal analysis. **Xingfu Liu:** Resources, Methodology. **Qian Zhou:** Resources, Methodology. **Yi-You Huang:** Methodology, Investigation. **Zhe Li:** Writing – review & editing, Writing – original draft, Visualization, Resources, Project administration. **Hai-Bin Luo:** Writing – review & editing, Supervision, Resources.

Acknowledgments

We acknowledge financial support from the Natural Science Foundation of China (Nos. 82373732, 22377023, 22307031, 81872727), Excellent Talent Team Project in Hainan Province (No. HNYT20250004), Hainan Provincial Natural Science Foundation of China (Nos. KJRC2023B10, 222RC556, 823CXTD375, 324MS018), Fundamental Research Funds for Hainan University (Nos. XTCX2022JKA01, KYQD(ZR)-21126, KYQD(ZR)-23003).

Supplementary materials

Supplementary material associated with this article can be found, in the online version, at doi:10.1016/j.cclet.2025.111236.

References

[1] J.W.H. Li, J.C. Vederas, Science 325 (2009) 161–165.
[2] K.F. Zhu, C. Yuan, Y.M. Du, et al., Military Med. Res. 10 (2023) 10.
[3] Q. Gong, J. Song, Y. Song, et al., Chin. Chem. Lett. 36 (2025) 110456.
[4] L.J. Gershell, J.H. Atkins, Nat. Rev. Drug Dis. 2 (2003) 321–327.
[5] M. Bissaro, M. Sturlese, S. Moro, Drug Discov. Today 25 (2020) 1693–1701.
[6] A. Fryszkowska, P.N. Devine, Curr. Opin. Chem. Biol. 55 (2020) 151–160.
[7] Z. Zhang, W. Tang, Acta Pharm. Sin. B 8 (2018) 721–732.
[8] Z. Zhang, M. Zhu, W. Tang, Curr. Pharm. Design 15 (2009) 2220–2235.
[9] D. Zhang, G. Luo, X. Ding, C. Lu, Acta Pharm. Sin. B 2 (2012) 549–561.
[10] M. Trunzer, B. Faller, A. Zimmerlin, J. Med. Chem. 52 (2009) 329–335.
[11] N. Harada, G.T. Miwa, J.S. Walsh, A.Y. Lu, J. Biol. Chem. 259 (1984) 3005–3010.
[12] C.J. Wenthur, R. Morrison, A.S. Felts, et al., J. Med. Chem. 56 (2013) 5208–5212.
[13] J.E. Gallant, S. Deresinski, Clin. Infect. Dis. 37 (2003) 944–950.
[14] T.M. Chapman, J.K. McGavin, S. Noble, Drugs 63 (2003) 1597–1608.
[15] J. Vamathevan, D. Clark, P. Czodrowski, et al., Nat. Rev. Drug Dis. 18 (2019) 463–477.
[16] N. Pillai, A. Dasgupta, S. Sudsakorn, J. Fretland, P.D. Mavroudis, Drug Dis. Today 27 (2022) 2209–2215.
[17] T.E. King, A. Pardo, M. Selman, Lancet 378 (2011) 1949–1961.
[18] F.J. Martinez, H.R. Collard, A. Pardo, et al., Nat. Rev. Dis. Primers 3 (2017) 17014.
[19] B. Ley, H.R. Collard, T.E. King Jr, Am. J. Resp. Crit. Care 183 (2011) 431–440.
[20] G. Raghu, S.Y. Chen, Q. Hou, W.S. Yeh, H.R. Collard, Eur. Respir. J. 48 (2016) 179–186.
[21] T. Zhang, C. Sun, S. Yang, et al., Chin. Chem. Lett. 35 (2024) 109248.
[22] G. Sgalla, B. Iovene, M. Calvello, et al., Resp. Res. 19 (2018) 32.
[23] A. Azuma, T. Nukiwa, E. Tsuboi, et al., Am. J. Resp. Crit. Care 171 (2005) 1040–1047.
[24] O. Distler, K.B. Highland, M. Gahlemann, et al., New Engl. J. Med. 380 (2019) 2518–2528.
[25] P. Spagnolo, J.A. Kropski, M.G. Jones, et al., Pharmacol Therapeut 222 (2021) 107798.
[26] The Idiopathic Pulmonary Fibrosis Clinical Research Network, New Engl. J. Med. 363 (2010) 620–628.
[27] M.K. Han, D.S. Bach, P.G. Hagan, et al., Chest 143 (2013) 1699–1708.
[28] D. Pissarnitski, Med. Res. Rev. 26 (2006) 369–395.
[29] D. Wu, T. Zhang, Y. Chen, et al., J. Med. Chem. 60 (2017) 6622–6637.
[30] A. Yamazaki, O. Moskvin, R.K. Yamazaki, Phosphorylation by cyclin-dependent protein kinase 5 of the regulatory subunit (Pγ) of retinal cGMP phosphodiesterase (PDE6): its implications in phototransduction, in: W. Baehr, K. Palczewski (Eds.), Advances in Experimental Medicine and Biology Photoreceptors and Calcium, Springer, Boston, 2002, pp. 131–153.
[31] J. Fiorito, J. Vendome, F. Saeed, et al., J. Med. Chem. 60 (2017) 8858–8875.
[32] Z. Li, X. Li, Y. Huang, et al., Proc. Natl. Acad. Sci. U. S. A. 17 (2020) 27381–27387.
[33] Z. Li, Y. Huang, Y. Wu, et al., J. Med. Chem. 62 (2019) 2099–2111.
[34] D. Wu, X. Zheng, R. Liu, et al., Acta Pharm. Sin. B 12 (2022) 1351–1362.
[35] J.L. Garcia Ruano, J. Alemán, C. Fajardo, A. Parra, Org. Lett. 7 (2005) 5493–5496.
[36] Z.J. Liu, J.T. Liu, Chem. Commun. (2008) 5233–5235.
[37] Z. Wang, X. Jiang, X. Zhang, et al., J. Med. Chem. 62 (2019) 4979–4990.
[38] D.P. Rotella, Nat. Rev. Drug Dis. 1 (2002) 674–682.
[39] T. Ukita, Y. Nakamura, A. Kubo, et al., Bioorg. Med. Chem. Lett. 13 (2003) 2341–2345.
[40] H. Mochida, M. Takagi, H. Inoue, et al., Eur. J. Pharm. 456 (2002) 91–98.
[41] N.K. Terrett, A.S. Bell, D. Brown, P. Ellis, Bioorg. Med. Chem. Lett. 6 (1996) 1819–1824.